η- and η'-mesic nuclei and $U_A(1)$ anomaly at finite density

Hideko Nagahiro,[1] Makoto Takizawa,[2] and Satoru Hirenzaki[3]
[1]*Research Center for Nuclear Physics(RCNP), Osaka University, Ibaraki, Osaka, 567-0047, Japan*
[2]*Showa Pharmaceutical University, Machida, Tokyo, 194-8543, Japan*
[3]*Department of Physics, Nara Women's University, Nara, 630-8506, Japan*
(Received 26 June 2006; published 20 October 2006)

We discuss theoretically the possibility of observing the bound states of the η and $\eta'(958)$ mesons in nuclei. We apply the NJL model to study the η and η' meson properties at finite density and calculate the formation cross sections of the η and η' bound states with the Green function method for (γ,p) reaction. We also discuss the experimental feasibility at photon facilities like SPring-8. The contributions due to the ω meson production are also included to obtain the realistic (γ,p) spectra. We conclude that we can expect to observe resonance peaks in (γ,p) spectra for the formation of meson bound states and we can deduce new information on η and η' properties at finite density. These observations are believed to be essential to know the possible mass shift of η' and deduce new information on the effective restoration of the $U_A(1)$ anomaly in the nuclear medium.

DOI: 10.1103/PhysRevC.74.045203 PACS number(s): 25.20.−x, 13.60.Le, 14.40.−n, 36.10.Gv

I. INTRODUCTION

Understanding the low-lying hadron structures from the viewpoint of the quark and gluon degrees of freedom is one of the most challenging problems in the quantum chromodynamics (QCD) because of its nonperturbative nature in the low-energy regime.

The lightest excitation on the QCD vacuum is the pion which is considered as a quark and an antiquark bound state in the pseudoscalar channel. Its mass is off-scale light compared with other hadrons. This can be understood by recognizing that the chiral symmetry is spontaneously broken in the QCD vacuum and the pion is the Nambu-Goldstone (NG) boson associated with the dynamical chiral symmetry breaking (DCSB). It is believed to be responsible for a large part of the constituent quark masses, which are introduced in the many constituent quark models. The effects of the explicit breaking of the chiral symmetry on the pion properties have been systematically studied using the effective lagrangian composed of the pion field. This approach is called the chiral perturbation theory (ChPT) [1]. The success of ChPT approach supports the importance of the DCSB in low-energy QCD.

When we start looking at the strange quark sector, we encounter another problem. The ninth heavier pseudoscalar meson is η' and its mass is much heavier than other octet pseudoscalar mesons. Weinberg showed that the mass of η' should be less than $\sqrt{3}m_\pi$ if $U_A(1)$ symmetry were not explicitly broken [2]. Thus the $U_A(1)$ symmetry must be broken. The key step to solve this $U_A(1)$ problem was to realize that $U_A(1)$ symmetry was explicitly broken by the quantum anomaly. In the following year, 't Hooft pointed out the relation between $U_A(1)$ anomaly and topological gluon configurations of QCD, i.e., instantons and showed that the interaction of light quarks and instantons breaks the $U_A(1)$ symmetry [3]. He also showed that such an interaction can be represented by a local $2N_f$ quark vertex, which is antisymmetric under flavor exchanges, in the dilute instanton gas approximation.

The effects of the $U_A(1)$ anomaly on the low-energy QCD have been extensively studied in the $1/N_c$ expansion approach [4]. In the $N_c \to \infty$ limit, the $U_A(1)$ anomaly is turned off and then the η and η' mesons become the ideal mixing states. The higher order effects of the $1/N_c$ expansion give rise to the flavor mixing between the η and η' mesons and push up the η' mass [5–8]. They were further discussed in the context of the ChPT [9] and the reasonable description of the nonet pseudoscalar mesons was obtained.

The $U_A(1)$ breaking $2N_f$ quark determinant interaction was introduced to the low-energy effective quark models of QCD. The low-lying meson properties have been studied [10–16] using the three-flavor version of the Nambu-Jona-Lasinio (NJL) model [17] with the Kobayashi-Maskawa-'t Hooft (KMT) determinant interaction [3,18]. It is further argued that the $U_A(1)$-breaking interaction gives rise to the spin-spin forces, which are important for light baryons [19–21].

It was observed by Witten that the instanton contribution scales as $\exp(-N_c)$ which seems to contradict the $1/N_c$ expansion approach, $m_{\eta'}^2 = O(1/N_c)$ [22]. A few years ago, Schäfer showed that the large N_c behavior of the instanton approach is consistent with the $1/N_c$ expansion approach if the instanton ensemble is stabilized by a classical repulsive core [23]. The use of the $U_A(1)$ breaking quark determinant interaction with the low-energy effective quark model of QCD in the mean field approximation seems to mimic the dilute instanton liquid picture, and therefore, we consider this approach is not inconsistent with the $1/N_c$ expansion approach.

The dynamics of instantons in the multi-instanton vacuum has been studied by many authors, either in the models or in the lattice QCD approach, and the widely accepted picture is that the QCD vacuum consists of small instantons of the size about 1/3 fm with the density of 1 instanton (or anti-instanton) per fm^4 [24]. In the instanton liquid model, the instanton plays a crucial role in understanding not only the $U_A(1)$ anomaly but also the spontaneous breaking of chiral symmetry itself.

In this paper, we consider the η and η' meson bound states in finite nuclei, i.e., η- and η'-mesic nuclei in order to investigate the change of the QCD vacuum structure at

finite density through the η and η' meson properties in the nuclear medium. Since the vacuum properties of η and η' are believed to have close relation to the QCD vacuum structure as described above, we can expect to have new information and much deeper insights on the QCD vacuum by knowing the η and η' meson properties at finite density, where the partial restoration of the DCSB is expected.

The η-mesic nucleus was studied by Haider and Liu [25] and Chiang, Oset, and Liu [26]. As for the formation reaction, the attempt to find the bound states by (π^+,p) reaction led to a negative result [27]. Recently, the η meson and light nuclei systems are studied experimentally [28] and also theoretically [29]. The experimental study in Ref. [28] claims the existence of the η-bound state in the light nucleus.

Recently, there are several very important developments in the research of the spontaneous breaking of chiral symmetry and its partial restoration at finite density by studying the hadronic systems, such as pionic atoms [30–32], η- and η'-mesic nuclei [33–38] and ω-mesic nuclei [33,34,39–41] in both of theoretical and experimental aspects. There is also a theoretical study on σ meson nuclear bound states based on SU(2) linear sigma model [42]. Especially, after a series of deeply bound pionic atom experiments [43,44], Suzuki *et al*. reported the quantitative determination of pion decay constant f_π in-medium [31] from the deeply bound pionic states in Sn isotopes [45] and stimulated many active researches of the partial restoration of chiral symmetry at finite density [30,32,46–48].

However, as for the behavior of the $U_A(1)$ anomaly in the nuclear medium, the present exploratory level is rather poor. Although some theoretical results have been reported, there exists no experimental information on the possible effective restoration of the $U_A(1)$ anomaly at finite density. In the context of the instanton dynamics, the mass of the η' at a nonzero baryon chemical potential was studied in the two color QCD [49]. As for the case of the finite temperature, the temperature dependence of the instanton density was calculated in Refs. [50–54]. In the low-energy effective model of QCD approach, Kunihiro studied the effects of the $U_A(1)$ anomaly on η' properties at finite temperature using the NJL model with the KMT term and showed the possible character changes of η' at $T \neq 0$ [55]. Theoretical predictions by other authors also supported the possible change of the η' properties at finite density as well as at finite temperature [56,57]. Experimental feasibilities to observe the η'-mesic nuclei were also studied in this context in our previous work in Ref. [37], where the in-medium η' properties were estimated quite roughly based on the results reported in Refs. [55–57]. In Ref. [38] further theoretial studies have been performed for η- and η'-nucleus systems with paying attention to the QCD axial U(1) problem.

In this study, we consider the η and η' meson properties in atomic nuclei and the structures of the η- and η'-mesic nuclei using the $SU(3)_f$ NJL model in order to get much deeper insights on the η' mass shifts and their relation to $U_A(1)$ anomaly effects and to get more quantitative results than our previous work [37]. We also propose the formation reaction of the η- and η'-mesic nuclei and discuss the possibility to produce the η- and η'-nucleus bound states. The η and η' properties in the medium should provide us important information on the QCD vacuum structure, especially on the effective restoration of the $U_A(1)$ symmetry in the nuclear medium.

This paper is organized as follows. In Sec. II, we will obtain the quark masses and the quark condensates in finite density using NJL model, and calculate the meson masses in-medium. In Sec. III, we will discuss the formations of mesic nuclei using the Green function method, and show the numerical results of the missing mass spectra of the (γ,p) reaction. Finally, Sec. IV is devoted to summary of this paper.

II. QUARK AND MESON MASSES IN NJL MODEL

We work with the following NJL model lagrangian density extended to three-flavor case:

$$\mathcal{L} = \mathcal{L}_0 + \mathcal{L}_4 + \mathcal{L}_6, \tag{1a}$$

$$\mathcal{L}_0 = \bar{\psi}\left(i\partial_\mu\gamma^\mu - \hat{m}\right)\psi, \tag{1b}$$

$$\mathcal{L}_4 = \frac{g_S}{2}\sum_{a=0}^{8}[(\bar{\psi}\lambda^a\psi)^2 + (\bar{\psi}\lambda^a i\gamma_5\psi)^2], \tag{1c}$$

$$\mathcal{L}_6 = g_D\{\det[\bar{\psi}_i(1-\gamma_5)\psi_j] + \text{h.c.}\}. \tag{1d}$$

Here the quark field ψ is a column vector in color, flavor and Dirac spaces and $\lambda^a (a = 0 \ldots 8)$ is the Gell-Mann matrices for the flavor U(3). The free Dirac Lagrangian $\mathcal{L}_0$ incorporates the current quark mass matrix $\hat{m} = \text{diag}(m_u, m_d, m_s)$ which breaks the chiral $U_L(3) \times U_R(3)$ invariance explicitly. $\mathcal{L}_4$ is a QCD motivated four-fermion interaction, which is chiral $U_L(3) \times U_R(3)$ invariant. The Kobayashi-Maskawa-'t Hooft determinant interaction $\mathcal{L}_6$ represents the $U_A(1)$ anomaly. It is a 3×3 determinant with respect to flavor with $i, j = \text{u, d, s}$.

Quark condensates $\langle\bar{q}q\rangle$ and constituent quark masses M_q are self-consistently determined by the gap equations in the mean field approximation,

$$\begin{aligned} M_u &= m_u - 2g_S\langle\bar{u}u\rangle - 2g_D\langle\bar{d}d\rangle\langle\bar{s}s\rangle, \\ M_d &= m_d - 2g_S\langle\bar{d}d\rangle - 2g_D\langle\bar{s}s\rangle\langle\bar{u}u\rangle, \\ M_s &= m_s - 2g_S\langle\bar{s}s\rangle - 2g_D\langle\bar{u}u\rangle\langle\bar{d}d\rangle, \end{aligned} \tag{2}$$

with

$$\begin{aligned} \langle\bar{q}q\rangle &= -\text{Tr}^{(c,D)}\left[iS_F^q(x=0)\right] \\ &= -\int\frac{d^4p}{(2\pi)^4}\text{Tr}^{(c,D)}\left[\frac{i}{p_\mu\gamma^\mu - M_q + i\epsilon}\right] \\ &= -2N_c\int^\Lambda\frac{d^3p}{(2\pi)^3}\frac{M_q}{E_q}(1 - n_p(T,\mu_q) - \bar{n}_p(T,\mu_q)). \end{aligned} \tag{3}$$

Here, the ultraviolet cutoff Λ is introduced to regularize the divergent integral and $\text{Tr}^{(c,D)}$ means trace in color and Dirac spaces. $E_q = \sqrt{\boldsymbol{p}_q^2 + M_q}$ is the on-shell energy of the quark and n_p and $\bar{n}_p$ are Fermi occupation numbers of quarks and

antiquarks, respectively, defined as

$$n_p(T,\mu_q) = \frac{1}{1+e^{(E_q-\mu_q)/T}}, \qquad \bar{n}_p(T,\mu_q) = \frac{1}{1+e^{(E_q+\mu_q)/T}}, \tag{4}$$

where T represents the temperature of the system and μ_q is the quark chemical potential. n_p and $\bar{n}_p$ depend on the momentum $\boldsymbol{p}_q$ through the energy E_q. For $T=0$, we can simply write Eqs. (4) as

$$n_p(0,\mu_q) = \theta(\mu_q - E_q), \qquad \bar{n}_p(0,\mu_q) = 0, \tag{5}$$

and by integrating them in momentum space we obtain the quark number density ρ_q as

$$\rho_q = \frac{1}{\pi^2}\left(\mu_q^2 - M_q^2\right)^{3/2}\theta(\mu_q - M_q). \tag{6}$$

To simulate the symmetric nuclear matter, we consider SU(2) symmetric quark matter defined as $\rho_u = \rho_d$, $\rho_s = 0$. In this case, the nucleon density ρ is defined as

$$\rho = \frac{1}{3}(\rho_u + \rho_d) = \frac{2}{\pi^2}\left(\mu_u^2 - M_u^2\right)^{3/2}\theta(\mu_u - M_u), \tag{7}$$

where $\mu_u = \mu_d$ and $M_u = M_d$. The NJL model at finite temperature and density has been reviewed in Ref. [58].

The pseudoscalar channel quark-antiquark scattering amplitudes,

$$\langle p_3, \bar{p}_4; \text{out}|p_1, \bar{p}_2; \text{in}\rangle = (2\pi)^4\delta^4(p_3 + p_4 - p_1 - p_2)\mathcal{T}_{q\bar{q}}, \tag{8}$$

are then calculated in the ladder approximation. We assume that $m_u = m_d$ so that the isospin symmetry is exact. In the η and η' channels, the explicit expression of $\mathcal{T}_{q\bar{q}}$ is

$$\mathcal{T}_{q\bar{q}} = -\begin{pmatrix}\bar{u}(p_3)\lambda^8 v(p_4)\\ \bar{u}(p_3)\lambda^0 v(p_4)\end{pmatrix}^T \begin{pmatrix}A(q^2) & B(q^2)\\ B(q^2) & C(q^2)\end{pmatrix} \times \begin{pmatrix}\bar{v}(p_2)\lambda^8 u(p_1)\\ \bar{v}(p_2)\lambda^0 u(p_1)\end{pmatrix}, \tag{9}$$

with

$$A(q^2) = \frac{2}{\det\mathbf{D}(q^2)}\{2\tilde{G}\,I^0(q^2) - G_8\}, \tag{10a}$$

$$B(q^2) = \frac{2}{\det\mathbf{D}(q^2)}\{-2\tilde{G}\,I^m(q^2) - G_m\}, \tag{10b}$$

$$C(q^2) = \frac{2}{\det\mathbf{D}(q^2)}\{2\tilde{G}I^8(q^2) - G_0\}, \tag{10c}$$

where $q = p_1 + p_2$ and $\tilde{G} = G_0G_8 - G_mG_m$, and

$$G_0 = \frac{1}{2}g_S - \frac{1}{3}(2\langle\bar{u}u\rangle + \langle\bar{s}s\rangle)g_D, \tag{11a}$$

$$G_8 = \frac{1}{2}g_S - \frac{1}{6}(\langle\bar{s}s\rangle - 4\langle\bar{u}u\rangle)g_D, \tag{11b}$$

$$G_m = -\frac{1}{3\sqrt{2}}(\langle\bar{s}s\rangle - \langle\bar{u}u\rangle)g_D. \tag{11c}$$

The quark-antiquark bubble integrals are defined by

$$I^0(q^2) = i\int\frac{d^4p}{(2\pi)^4} \times \mathrm{Tr}^{(c,f,D)}[S_F(p)\lambda^0 i\gamma_5 S_F(p+q)\lambda^0 i\gamma_5], \tag{12a}$$

$$I^8(q^2) = i\int\frac{d^4p}{(2\pi)^4} \times \mathrm{Tr}^{(c,f,D)}[S_F(p)\lambda^8 i\gamma_5 S_F(p+q)\lambda^8 i\gamma_5], \tag{12b}$$

$$I^m(q^2) = i\int\frac{d^4p}{(2\pi)^4} \times \mathrm{Tr}^{(c,f,D)}[S_F(p)\lambda^0 i\gamma_5 S_F(p+q)\lambda^8 i\gamma_5]. \tag{12c}$$

In the calculations of the quark loop integrals, we have applied standard techniques of thermal field theory, i.e., the imaginary-time formalism and we have introduced the same three-momentum cutoff used in the gap equations (2) and (3).

The 2×2 matrix $\mathbf{D}$ is given by

$$\mathbf{D}(q^2) = \begin{pmatrix}D_{11}(q^2) & D_{12}(q^2)\\ D_{21}(q^2) & D_{22}(q^2)\end{pmatrix}, \tag{13}$$

with

$$D_{11}(q^2) = 2G_0I^0(q^2) + 2G_mI^m(q^2) - 1, \tag{14a}$$

$$D_{12}(q^2) = 2G_0I^m(q^2) + 2G_mI^8(q^2), \tag{14b}$$

$$D_{21}(q^2) = 2G_8I^m(q^2) + 2G_mI^0(q^2), \tag{14c}$$

$$D_{22}(q^2) = 2G_8I^8(q^2) + 2G_mI^m(q^2) - 1. \tag{14d}$$

From the pole positions of the scattering amplitude Eq. (9), the η-meson mass m_η and the η'-meson mass $m_{\eta'}$ are determined.

The scattering amplitude Eq. (9) can be diagonalized by the rotation in the flavor space

$$\mathcal{T}_{q\bar{q}} = -\begin{pmatrix}\bar{u}(p_3)\lambda^8 v(p_4)\\ \bar{u}(p_3)\lambda^0 v(p_4)\end{pmatrix}^T \mathbf{T}_\theta^{-1}\mathbf{T}_\theta \begin{pmatrix}A(q^2) & B(q^2)\\ B(q^2) & C(q^2)\end{pmatrix}\mathbf{T}_\theta^{-1} \times\mathbf{T}_\theta \begin{pmatrix}\bar{v}(p_2)\lambda^8 u(p_1)\\ \bar{v}(p_2)\lambda^0 u(p_1)\end{pmatrix}, \tag{15}$$

$$= -\begin{pmatrix}\bar{u}(p_3)\lambda^\eta v(p_4)\\ \bar{u}(p_3)\lambda^{\eta'} v(p_4)\end{pmatrix}^T \begin{pmatrix}D^\eta(q^2) & 0\\ 0 & D^{\eta'}(q^2)\end{pmatrix} \times \begin{pmatrix}\bar{v}(p_2)\lambda^\eta u(p_1)\\ \bar{v}(p_2)\lambda^{\eta'} u(p_1)\end{pmatrix}, \tag{16}$$

with $\lambda^\eta \equiv \cos\theta\lambda^8 - \sin\theta\lambda^0$, $\lambda^{\eta'} \equiv \sin\theta\lambda^8 + \cos\theta\lambda^0$ and

$$\mathbf{T}_\theta = \begin{pmatrix}\cos\theta & -\sin\theta\\ \sin\theta & \cos\theta\end{pmatrix}. \tag{17}$$

The rotation angle θ is determined by

$$\tan 2\theta = \frac{2B(q^2)}{C(q^2) - A(q^2)}. \tag{18}$$

Note that θ therefore depends on q^2. At $q^2 = m_\eta^2$, θ represents the mixing angle of the λ^8 and λ^0 components in the η-meson state. In the usual effective pseudoscalar meson Lagrangian approaches, the η and η' mesons are analyzed using the q^2-independent $\eta - \eta'$ mixing angle. Because of the

TABLE I. Input parameters determined in Ref. [59] and calculated results in vacuum in three-flavor NJL model.

Input parameters	Calculated results [MeV]	
$\Lambda = 602.3$ [MeV]	$M_{u,d} = 367.6$	$f_\pi = 92.4$
$g_S\Lambda^2 = 3.67$	$M_s = 549.5$	$m_\pi = 135.0$
$g_D\Lambda^5 = -12.36$	$\langle\bar{u}u\rangle^{1/3} = -241.9$	$m_\eta = 514.8$
$m_{u,d} = 5.5$ [MeV]	$\langle\bar{s}s\rangle^{1/3} = -257.7$	$m_{\eta'} = 957.7$
$m_s = 140.7$ [MeV]		

q^2-dependence, θ cannot be interpreted as the $\eta - \eta'$ mixing angle. The origin of the q^2-dependence is that the η and η' mesons have the internal structures.

We obtain the dynamical quark and meson masses in vacuum as compiled in Table I with the input parameters determined in Ref. [59]. In Ref. [59], the four model parameters, namely, cutoff Λ, four-quark coupling constant g_S, six-quark coupling constant g_D and the current s-quark mass m_s have been fixed so as to reproduce the observed values of the pion, kaon, η' masses and the pion decay constant, while the current u, d-quark mass has been fixed at 5.5 MeV, which has been taken from the results of the chiral perturbation theory and QCD sum rule approaches. This parameter set gives an η mass of $m_\eta = 514.8$ MeV, which is about 6% smaller than the observed value $m_\eta = 547.75$ MeV. One is able to fit the mass of η instead of the η'. The reason why we have used the present parameter set is just we are more interested in the η'-mesic nucleus than the η-mesic nucleus in this article because we consider that the former is more suitable for observing the finite density effect of the $U_A(1)$ anomaly.

In this paper, we investigate the finite density effects on the meson mass spectra for the following three cases with the different strengths g_D of the determinant KMT interaction as

$$\begin{aligned} &\text{(a) } g_D(\rho) = g_D \\ &\text{(b) } g_D(\rho) = 0 \\ &\text{(c) } g_D(\rho) = g_D \exp[-(\rho/\rho_0)^2], \end{aligned} \tag{19}$$

where g_D is the vacuum strength of the determinant interaction as shown in Table I. The $g_D(\rho)$ has no density dependence for cases (a) and (b). In case (a), the meson vacuum properties are well reproduced as shown in Table I, while there are no anomaly effects in case (b). For $g_D = 0$ case, we use slightly different parameter set as shown in Table I in Ref. [60] to reproduce the meson masses and the pion decay constant in vacuum without anomaly effect. In case (c), we simply assume the density dependence of g_D as this form in order to examine the medium effect due to density dependence of g_D itself on the meson mass spectra in finite density.

Here it may be interesting for our study to notice that there are theoretical suggestions about possible density dependence of g_D [61,62]. In Ref. [62], the effective coupling constant of the instanton-induced interaction is suggested to have chemical potential dependence for $N_f = 2$ systems. For $N_f = 3$ systems, we can expect to have the similar μ dependence, though it is not easy to show explicitly. We are interested in studying the effect of such density dependence discussed in Ref. [62] on meson mass spectra as future works.

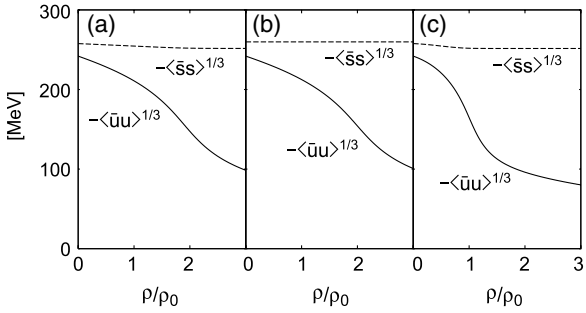

FIG. 1. Density dependence of the quark condensates in the SU(2) symmetric matter, $\rho_u = \rho_d$ and $\rho_s = 0$, where $\langle\bar{u}u\rangle = \langle\bar{d}d\rangle$. Three panels correspond to the cases (a), (b), and (c) defined in Eq. (19), respectively. The nucleon density ρ is defined in Eq. (7) and ρ_0 is the normal nuclear density $\rho_0 = 0.17$ fm^{-3}.

In Fig. 1, we show the calculated quark condensates as functions of density for three types of $g_D(\rho)$ defined in Eq. (19). In case (b), we have switched off the effect of the instanton-induced flavor mixing interaction and therefore the s-quark condensate has not changed in the SU(2) symmetric matter. The absolute values of the u,d-quark condensate decreases significantly faster in case (c) than in case (a) when the density goes up. It means that the contribution of the instanton-induced interaction on the u,d-quak condensate is sizable.

In Fig. 2, we show the calculated density dependence of the meson mass spectra for three cases defined in Eq. (19). In the case of constant g_D (a), we find that the mass of η' decreases rapidly as a function of the density, while the masses of π and η gradually increase. The instanton-induced interaction is repulsive for the flavor singlet $\bar{q}q$ channel and the effective coupling strength is $g_D(\langle\bar{u}u\rangle + \langle\bar{d}d\rangle + \langle\bar{s}s\rangle)/3$. Since the absolute values of the quark condensates decrease as the density increase, the effective repulsive interaction in the flavor singlet $\bar{q}q$ channel becomes small as the density increases. That is the reason why the η' mass decrease. In Fig. 2(b), we find that π and η are degenerate completely and their masses increase gradually as density, and the mass of η' has no density dependence without the $U_A(1)$ anomaly effects. Without the $U_A(1)$ anomaly effects,

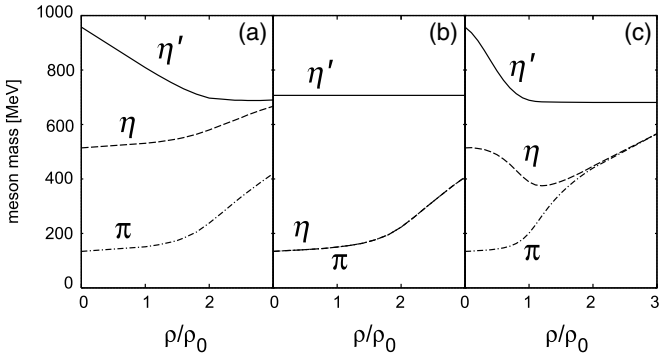

FIG. 2. Density dependence of the meson mass spectra. Three panels corresponds to the cases (a), (b), and (c) defined in Eq. (19), respectively. The nucleon density ρ is defined in Eq. (7) and ρ_0 is the normal nuclear density $\rho_0 = 0.17$ fm^{-3}.

the η' is the ideal mixing state, i.e., the pure $\bar{s}s$, and therefore no density dependence in the SU(2) symmetric matter with $\mu_s = 0$. It should be mentioned that the masses of η and η' at $\rho = 0$ are not reproduced in this case. As shown in Fig. 2(c), if the g_D has density dependence as case (c) in Eq. (19), we can expect mass reduction of both η and η' mesons up to around $\rho = \rho_0$.

It is interesting to compare our results in Fig. 2 with those obtained in Ref. [38], where the quark-meson coupling model (QMC) was used to obtain the mass-shift for given mixing angles. The results in Table 1 of Ref. [38] show that the both masses of η and η' decrease in medium at normal nuclear density (defined as $\rho_0 = 0.15$ fm^{-3} in Ref. [38]) for all cases considered there. These results are not consistent to our results of case (a) where the η mass slightly increases at the normal nuclear density. Our results of case (c) are qualitatively consistent to those in Ref. [38] and predict the mass reduction of η and η' mesons in medium at normal nuclear density, however, the sizes of the mass shift are significantly different in these results. The origin of the discrepancies in theoretical calculations are not clear, however, we believe that this fact indicates the significant importantce of experimental information.

Here, in order to see the effects of the species of the matter to the calculated results, we compare the results in the SU(2) symmetric matter with those in the SU(3) symmetric matter, $\rho_u = \rho_d = \rho_s$, in Fig. 3. In Fig. 3, the strength of the determinant interaction is fixed to be constant as case (a) in Eq. (19). We get same results as those obtained in Ref. [60] in SU(3) case, and find that the differences between the calculated results in SU(2) and that of SU(3) are less than 10% at normal nuclear density ρ_0.

III. FORMATION SPECTRA OF MESIC NUCLEI

In previous section, we discuss the possible changes of the meson masses due to the medium effects. If such mass changes occur in the nuclear medium, we can translate these effects into the potential forms. We estimate the real parts of the η- and η'-nucleus optical potentials based on the calculated

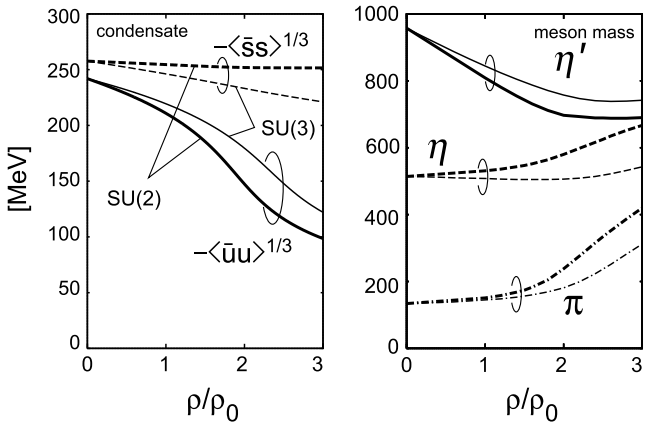

FIG. 3. Density dependence of the quark condensates (left panel) and the meson masses (right panel) are shown for the SU(2) symmetric matter (thick lines) and the SU(3) symmetric matter (thin lines). The nucleon density ρ is defined in Eq. (7) and ρ_0 is the normal nuclear density $\rho_0 = 0.17$ fm^{-3}.

their masses at finite density by the NJL model. The optical potential $U(r)$ can be written as

$$U(r) = V(r) + iW(r), \tag{20}$$

where V and W indicate the real and the imaginary parts of the optical potential, respectively. The mass term in the Klein-Gordon equation for the η and η' mesons can be rewritten at finite density as

$$m_0^2 \to m^2(\rho) = (m_0 + \Delta m(\rho))^2 \sim m_0^2 + 2m_0\Delta m(\rho), \tag{21}$$

where m_0 is the calculated meson mass in vacuum and $m(\rho)$ the meson mass at density ρ. The mass shift $\Delta m(\rho)$ is defined as $\Delta m(\rho) = m(\rho) - m_0$ and is $\Delta m(0) = 0$. Thus, we can interpret the $\Delta m(\rho)$ as the strength of the real part of the optical potential, and in this paper we write $V(r)$ as

$$V(r) = \Delta m(\rho_0)\frac{\rho(r)}{\rho_0}, \tag{22}$$

using the meson mass shifts at normal nuclear density ρ_0. Here $\rho(r)$ is the nuclear density distribution, which is assumed to be of an empirical Woods-Saxon form as

$$\rho(r) = \frac{\rho_0}{1 + \exp\left(\frac{r-R}{a}\right)}, \tag{23}$$

where $R = 1.18A^{\frac{1}{3}} - 0.48$ fm and $a = 0.5$ fm with the nuclear mass number A.

From the calculated results shown in Fig. 2, we can deduce the real part of the η- and η'-nucleus optical potential as defined in Eq. (22). We show the real parts of the optical potentials in Fig. 4 for all these cases defined in Eq. (19). We find that the sign and strength of the real part of the optical potential strongly depends on the anomaly effects at finite ρ. The potential of η' is attractive for cases (a) and (c), and its strength depends on the density dependence of $g_D(\rho)$. As we can see in Fig. 4(b), no real potential is expected for η' meson for $g_D = 0$ case. As for η-nucleus optical potential, even the sign of the real potential is changed by the density dependence of $g_D(\rho)$ as shown in Figs. 4(a) and 4(c). For no anomaly case (b), η meson degenerates with pion and the real potential is slightly repulsive. Thus, we confirm that we can expect to

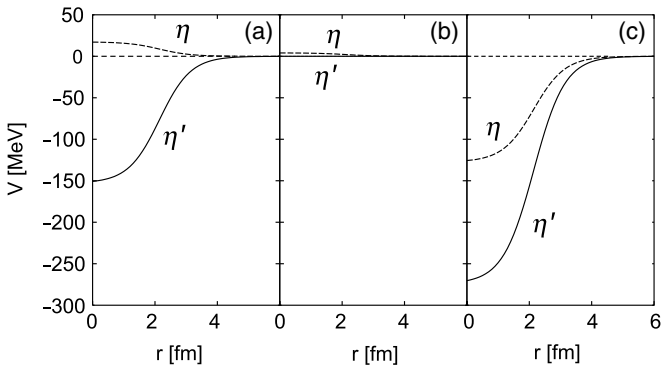

FIG. 4. Real parts of the η- and $\eta'-{}^{11}$B optical potentials determined by the meson mass shifts of NJL model in SU(2) symmetric matter as defined in Eq. (22). Three panels correspond to the cases (a), (b), and (c) defined in Eq. (19), respectively.

obtain the information on $U_A(1)$ anomaly by knowing the η and η' meson properties at finite ρ.

The strength of the imaginary potential of meson and nucleus is estimated separately since it is extremely difficult to evaluate it using NJL model. For the η meson, we estimate the strength of the imaginary potential based on the results obtained in Refs. [35] assuming the $N^*(1535)$ dominance in the ηN channel, and take as

$$W(r) = -40\frac{\rho(r)}{\rho_0}\ [\mathrm{MeV}]. \tag{24}$$

As for the η' nucleus optical potential, we can estimate $W(r)$ from analysis of $\gamma p \to \eta' p$ data [63]. Since they included only $N^*(1535)$ as a baryon resonance in the analysis of the η' formation reaction and determined $\eta' N N^*(1535)$ coupling strength, we can easily calculate the η' self-energy in the medium in analogy with the Δ-hole model for the π-nucleus system as

$$\begin{aligned} U_{\eta'} &\sim \frac{g^2}{2m_{\eta'}}\frac{\rho}{m_{\eta'} + M_N - M_{N^*} + i\Gamma_{N^*}/2} \\ &= (+77 - 8i)\frac{\rho}{\rho_0}\ [\mathrm{MeV}]. \end{aligned} \tag{25}$$

We consider the reasonable running range is from -5 MeV to -20 MeV for the strength of the imaginary part of the η' nucleus optical potential based on this evaluation in Eq. (25) as in Ref. [37]. The η'-nucleus bound states were calculated theoretically before in Ref. [64] where the widths of the η'-mesic nuclear states were not evaluated.

We should mention here that the evaluation in Eq. (25) provides the repulsive real part, which is opposite to the evaluation from the η' mass shift, since we consider only $N^*(1535)$ resonance with the mass $M_{N^*} < m_{\eta'} + M_N$ as an intermediate states. By the (γ,p) experiments proposed in this paper, we can expect to distinguish these potentials and to determine the sign and strength of the η'-nucleus optical potential.

In order to observe meson-nucleus bound states experimentally, we consider missing mass spectroscopy [65], which was proved to be a powerful tool for the meson bound states formation in the studies of deeply bound pionic states [66]. In this spectroscopy, one observes an emitted particle in a final state, and obtains the double differential cross section $d^2\sigma/d\Omega/dE$ as a function of the emitted particle energy. As discussed in Refs. [37,67–69], we think that the (γ, p) reaction with GeV photon beam is one of the appropriate reactions for our purpose and it can be performed in existing facilities like SPring-8. We consider the (γ,p) reactions for the η- and η'-mesic nuclei formation.

We choose the incident photon energy as $E_\gamma = 2.7$ GeV, which is the beam energy accessible at SPring-8, and choose ^{12}C as a target nucleus as in Ref. [37]. We use the Green function method [70] to calculate the formation cross sections as

$$\left(\frac{d^2\sigma}{d\Omega dE}\right)_{A(\gamma,p)\eta,\eta'\otimes(A-1)} = \left(\frac{d\sigma}{d\Omega}\right)^{\mathrm{Lab}}_{p(\gamma,p)\eta,\eta'} \times \sum_f S(E), \tag{26}$$

where $S(E)$ is the nuclear response function and $\left(\frac{d\sigma}{d\Omega}\right)^{\mathrm{Lab}}_{p(\gamma,p)\eta,\eta'}$ are the elementary cross sections in the laboratory frame for the η and η' meson production. The elementary cross section for η' production is estimated to be 150 nb/sr using the data of SAPHIR collaboration [71] and their analysis [72]. As for the η production process, we take the same value for the elementary cross section as $\left(\frac{d\sigma}{d\Omega}\right)^{\mathrm{Lab}}_{p(\gamma,p)\eta} = 150$ nb/sr based on the data at SPring-8 [73] which show the similar production rate for both mesons in a test experiment in the preparation stage. We sum up all (proton-hole)$\otimes$(meson-particle) configurations in the final state to get the total cross section in Eq. (26).

To calculate the response function $S(E)$, we use the Green function $G(E;\vec{r},\vec{r'})$ defined as [70]

$$G(E;\vec{r},\vec{r'}) = \langle p^{-1}|\phi(\vec{r})\frac{1}{E - H + i\epsilon}\phi^\dagger(\vec{r'})|p^{-1}\rangle, \tag{27}$$

where $\phi^\dagger$ is the meson creation operator and $|p^{-1}\rangle$ is a proton hole state. The Hamiltonian H contains the meson-nucleus optical potential U. We can rewrite Eq. (27) in a simple expression as [70]

$$G(E;\vec{r},\vec{r'}) = \sum_{l,m} Y^*_{l,m}(\hat{r})Y_{l,m}(\hat{r'})G_l(E;r,r') \tag{28}$$

$$G_l(E;r,r') = -2mku_l(k,r_<)v_l^{(+)}(k,r_>), \tag{29}$$

where u_l and $v_l^{(+)}$ are the radial part of the regular and outgoing solutions of equation of motion, respectively. Using the Green function, the response function can be expressed as

$$\begin{aligned} S(E) = -\frac{1}{\pi}Im\sum_{J,M,m_s}\int d^3r d\sigma d^3r' d\sigma' \\ \times f^\dagger(\vec{r},\sigma)G(E;r,r')f(\vec{r'},\sigma). \end{aligned} \tag{30}$$

Here, we define $f(\vec{r},\sigma)$ as

$$f(\vec{r},\sigma) = \chi^*_f(\vec{r})\xi^*_{\frac{1}{2},m_s}(\sigma)[Y^*_l(\hat{r})\otimes\psi_{j_p}(\vec{r},\sigma)]_{JM}\chi_i(\vec{r}), \tag{31}$$

where χ_i and χ_f denote the projectile and the ejectile distorted waves, respectively, ψ is the proton-hole wave function and ξ is the spin wave function introduced to count possible spin directions of the proton in the target nucleus. The distorted waves χ_i and χ_f are evaluated by using the eikonal approximation as in Ref. [37].

In Fig. 5, we show the calculated spectra of ^{12}C$(\gamma$,p) reaction for the η' meson formation as functions of the excited energy which are defined as

$$E_{ex} = m_{\eta'} - B_{\eta'} + [S_p(j_p) - S_p(p_{3/2})], \tag{32}$$

where $B_{\eta'}$ is the η' binding energy and S_p the proton separation energy. The η' production threshold energy E_0 is indicated in the figure by the vertical dashed line. The real part of the optical potential is evaluated for case (a) in Eq. (19) which has around -150 MeV depth at nuclear center as can be seen in Fig. 4(a). The spectra are calculated for (upper panel) $W_0 = -5$ MeV and (lower panel) $W_0 = -20$ MeV cases where the imaginary potential is written as $W(r) = W_0\rho(r)/\rho_0$. We also show the dominant subcomponents of the spectra in Fig. 5. As we can see from these figures, we can expect to observe the peak structures in the spectra due to the formation of the η'-mesic nucleus even

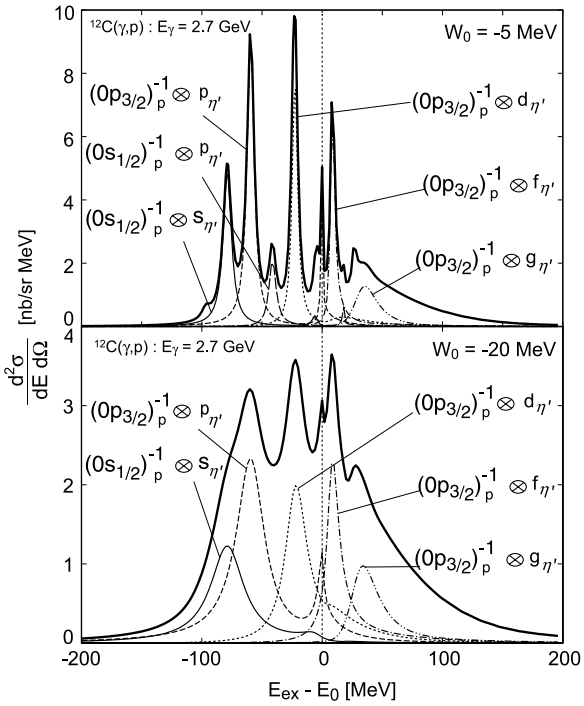

FIG. 5. The calculated spectra of the $^{12}C(\gamma,p)^{11}B \otimes \eta'$ reaction at $E_\gamma = 2.7$ GeV are shown as functions of the excited energy E_{ex} defined in the text. E_0 is the η' production threshold energy. The real part of the η'-nucleus optical potential is evaluated for case (a) in Eq. (19). The imaginary part of the potential is assumed to be $W(r) = -5\rho(r)/\rho_0$ [MeV] (upper panel) and $W(r) = -20\rho(r)/\rho_0$ [MeV] (lower panel). The total spectra are shown by the thick solid line, and the dominant contributions of subcomponents are shown by dotted and dashed lines as indicated in the figures.

in the case with the relatively large imaginary potential, and we can expect to deduce the magnitude of the η' mass shift at finite nuclear density from the observed spectra. The evaluated imaginary part of the η'-nucleus potential is small enough and the resonance peaks are expected to be clearly separated each other. Hereafter, we show the calculated spectra of the η'-mesic nuclei formation only for $W_0 = -20$ MeV cases.

In Figs. 6 and 7, we show the (γ,p) spectra for wider energy region including both η and η' production to see the anomaly effects in the whole (γ,p) spectra simultaneously. To provide realistic spectra, we include the contributions due to ω meson production processes, which exist between η and η' contributions. As the ω-nucleus interaction, we apply the results obtained by two theory groups reported in Refs. [40] and [41]. We should mention here that the ω-nucleus interaction at threshold in Ref. [40] is attractive, while that in Ref. [41] is repulsive. Hence, we use both interactions to evaluate the contribution of ω meson.

In Fig. 6, we show the spectra including the contribution due to the formation of the ω mesic nuclei with the attractive potential reported in Ref. [40]. We can see the significant mass reduction of the η' meson in nuclear medium in Fig. 6(a), while in Fig. 6(b) we only see the simple quasifree η' formation spectrum without $U_A(1)$ anomaly effect. In the case with the density dependent g_D in Fig. 6(c), we can see the mass

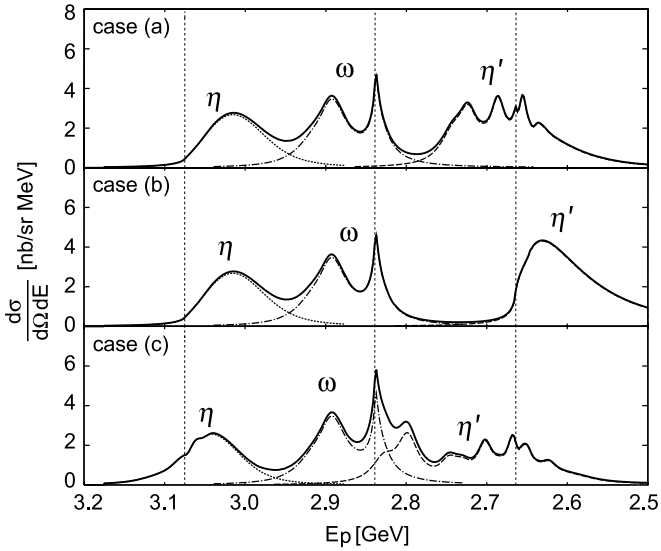

FIG. 6. The calculated spectra of the $^{12}C(\gamma,p)$ reactions for the η, ω, η' mesic nucleus formation at $E_\gamma = 2.7$ GeV are shown as functions of the emitted proton energies in final states. The three cases (a), (b), and (c) for g_D defined in Eq. (19) are considered. The vertical dashed lines indicate the production thresholds of the η, ω and η' mesons. The contributions from the η, ω and η'-mesic nuclei are shown by dotted, dash-dotted and dashed lines, respectively. The imaginary part of the η'-nucleus optical potential is $W(r) = -20\rho(r)/\rho_0$ MeV. The ω-nucleus optical potential obtained in Ref. [40] is used and is attractive.

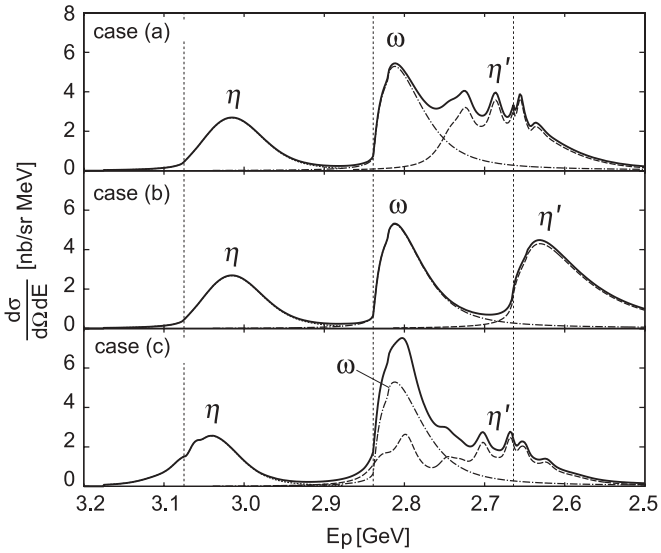

FIG. 7. The calculated spectra of the $^{12}C(\gamma,p)$ reactions for the η, ω, η' mesic nucleus formation at $E_\gamma = 2.7$ GeV are shown as functions of the emitted proton energies in final states. The three cases (a), (b), and (c) for g_D defined in Eq. (19) are considered. The vertical dashed lines indicate the production thresholds of the η, ω and η' mesons. The contributions from the η, ω and η'-mesic nuclei are shown by dotted, dash-dotted and dashed lines, respectively. The imaginary part of the η'-nucleus optical potential is $W(r) = -20\rho(r)/\rho_0$ MeV. The ω-nucleus optical potential obtained in Ref. [41] is used and is repulsive.

reduction of both the η and η' mesons. Especially, even below the ω production threshold, we can see the finite contributions of the η' mesic nuclei formation to the spectrum as the consequences of the large η' mass reduction in the case with the density dependent g_D defined as (c) in Eq. (19). For the η mesic nuclei production, it is hardly to see the differences between the cases with (a) the constant g_D and (c) the density dependence g_D, due to the large momentum transfer for the η mesic nuclei formation with the incident photon energy $E_\gamma = 2.7$ GeV considered in this paper. At this energy, the contributions from higher partial waves of quasi-free η meson production are so large that those from the bound η states hardly affect the total spectrum. Furthermore, we should make a comment on the η mesic nuclei that, in order to see the anomaly effect clearly, we have not considered any contributions from resonances like $N^*(1535)$ in this paper in the estimation of the real part of the η-nucleus optical potential, whose contribution is known to be important on the η-nucleon system. The detailed discussions of the η-mesic nuclei with the $N^*(1535)$ resonance are reported in Refs. [35,69]. The calculated contribution of the ω channel in Fig. 6 is essentially the same as that reported in Ref. [67].

Similarly, in Fig. 7 we show the spectra with the ω mesic nuclei with the repulsive potential predicted in Ref. [41]. In this case, the contribution of the quasifree ω formation locates the same energy region with the bound η' in the cases (a) and, especially (c) in Fig. 7. In Fig. 7(b), we can only see simple three peaks corresponding the quasi-free η, ω and η' mesons in the spectrum.

As for the background, which is very important to discuss experimental feasibility, is evaluated by using the experimental data taken by LEPS collaboration at SPring-8 recently [73]. That was a test experiment in the preparation stage for the observation of the ω mesic nuclei by the (γ,p) reaction, which used the same kinematics proposed in this paper and observed the background proton emission rate from Carbon target including energy region for the η' meson production [73]. We can roughly estimate the order of magnitude of the background proton cross section as to be 10–100 [nb/sr MeV] in the η' formation region. Thus, we estimate the signal over noise ratio is around $S/N \sim 1/10$. We think the absolute magnitude of the calculated formation cross section is reasonably large and the spectra are expected to be observed in future experiments at SPring-8 [73].

IV. CONCLUSIONS

We have investigated the possible observation of the effective restoration of the $U_A(1)$ anomaly at finite density by formations of the η- and η'-mesic nuclei. Especially, since the heavy η' meson mass is considered to be generated from the $U_A(1)$ anomaly effect, we can expect to observe clearly the anomaly effect in medium in the η' channel.

In order to evaluate more quantitative magnitude of the meson mass changes due to the medium effects and to obtain deeper insights on $U_A(1)$ anomaly effects than Ref. [37], we adopted the Nambu-Jona-Lasinio (NJL) model with the Kobayashi-Maskawa-'t Hooft (KMT) interaction, and calculated the meson masses in finite density with three different coupling strengths of the KMT interaction. We obtained significant η' mass changes even at normal nuclear density due to the effective restoration of the $U_A(1)$ anomaly. In the finite density calculations, we have substituted the SU(2) symmetric constituent quark matter for the symmetric nuclear matter. Although the NJL model doesn't confine quarks, it is a good effective model which can describe the low energy QCD phenomena, i.e., the properties of light pseudoscalar mesons rather well after fixing the model parameters appropriately. Even the NJL model has some shortcomings, we think it is meaningful to apply the model in this exploratory level to clarify the physics of $\eta'(958)$ mesic nuclei and $U_A(1)$ anomaly at finite density.

To investigate the experimental feasibility, we calculated formation cross sections of the η- and η'-mesic nuclei with (γ,p) reaction. We found that the calculated cross section has reasonably large magnitude, and the (γ,p) reaction with GeV photon beam, which can be provided in existing facilities like SPring-8, is an appropriate reaction for our purpose. We conclude that we can expect to observe the η' mass reduction clearly in this reaction, and to obtain new information on the $U_A(1)$ anomaly at finite density.

The present evaluation is the first theoretical results for the formation reaction of the η- and η'-mesic nuclei based on the NJL model results to know the behavior of $U_A(1)$ anomaly in the medium. We believe that the present theoretical results is much important to stimulate both theoretical and experimental activities to study the $U_A(1)$ anomaly at finite density and to obtain the deeper insights of QCD symmetry breaking pattern and the meson mass spectrum.

ACKNOWLEDGMENTS

We would like to thank D. Jido and M. Oka for useful comments. We also thank N. Muramatsu for valuable discussions on the latest data of the (γ,p) reactions at SPring-8. H.N. and S.H. also thank T. Hatsuda for valuable discussions at the early stage of this work. H.N. thanks A. Hosaka for useful comments and discussions. One of the authors (H.N.) is supported by research grants of the Japan Society for the Promotion of Science (JSPS) for Young Scientists. This work is partly supported by Grants-in-Aid for scientific research of MonbuKagakushou and Japan Society for the Promotion of Science [No. 16540254 (S.H.) and No. 18·8661 (H.N.)].

[1] J. Gasser and H. Leutwyler, Ann. Phys. (NY) **158**, 142 (1984).
[2] S. Weinberg, Phys. Rev. D **11**, 3583 (1975).
[3] G. 't Hooft, Phys. Rev. Lett. **37**, 8 (1976); Phys. Rev. D **14**, 3432 (1976).
[4] G. 't Hooft, Nucl. Phys. **B72**, 461 (1974).
[5] C. Rosenzweig, J. Schechter, and C. G. Trahern, Phys. Rev. D **21**, 3388 (1980).
[6] P. Di Vecchia and G. Veneziano, Nucl. Phys. **B171**, 253 (1980).
[7] K. Kawarabayashi and N. Ohta, Nucl. Phys. **B175**, 477 (1980).
[8] P. Nath and R. Arnowitt, Phys. Rev. D **23**, 473 (1981).

[9] H. Leutwyler, Nucl. Phys. B Proc. Suppl. **64**, 223 (1998).
[10] T. Kunihiro and T. Hatsuda, Phys. Lett. **B206**, 385 (1988); **210**, 278 (1988); T. Hatsuda and T. Kunihiro, Z. Phys. C **51**, 49 (1991).
[11] V. Bernard, R. L. Jaffe, and U.-G. Meissner, Nucl. Phys. **B308**, 753 (1988).
[12] Y. Kohyama, K. Kubodera, and M. Takizawa, Phys. Lett. **B208**, 165 (1988); M. Takizawa, K. Tsushima, Y. Kohyama, and K. Kubodera, Prog. Theor. Phys. **82**, 481 (1989); Nucl. Phys. **A507**, 611 (1990).
[13] H. Reinhardt and R. Alkofer, Phys. Lett. **B207**, 482 (1988); R. Alkofer and H. Reinhardt, Z. Phys. C **45**, 275 (1989).
[14] S. Klimt, M. Lutz, U. Vogl, and W. Weise, Nucl. Phys. **A516**, 429 (1990).
[15] M. Takizawa and M. Oka, Phys. Lett. **B359**, 210 (1995); **364**, 249(E) (1995).
[16] Y. Nemoto, M. Oka, and M. Takizawa, Phys. Rev. D **54**, 6777 (1996); M. Takizawa, Y. Nemoto, and M. Oka, *ibid.* **55**, 4083 (1997).
[17] Y. Nambu and G. Jona-Lasinio, Phys. Rev. **122**, 345 (1961); **124**, 246 (1961).
[18] M. Kobayashi and T. Maskawa, Prog. Theor. Phys. **44**, 1422 (1970); M. Kobayashi, H. Kondo, and T. Maskawa, *ibid.* **45**, 1955 (1971).
[19] E. V. Shuryak and J. L. Rosner, Phys. Lett. **B218**, 72 (1989).
[20] M. Oka and S. Takeuchi, Phys. Rev. Lett. **63**, 1780 (1989); Nucl. Phys. **A524**, 649 (1991); S. Takeuchi and M. Oka, Phys. Rev. Lett. **66**, 1271 (1991).
[21] O. Morimatsu and M. Takizawa, Nucl. Phys. **A554**, 635 (1993).
[22] E. Witten, Nucl. Phys. **B149**, 285 (1979).
[23] T. Schäfer, Phys. Rev. D **66**, 076009 (2002).
[24] For a review, T. Schäfer, and E. V. Shuryak, Rev. Mod. Phys. **70**, 323 (1998), and references therein.
[25] Q. Haider and L. C. Liu, Phys. Lett. **B172**, 257 (1986); L. C. Liu and Q. Haider, Phys. Rev. C **34**, 1845 (1986).
[26] H. C. Chiang, E. Oset, and L. C. Liu, Phys. Rev. C **44**, 738 (1991).
[27] R. E. Chrien *et al.*, Phys. Rev. Lett. **60**, 2595 (1988).
[28] M. Pfeiffer *et al.*, Phys. Rev. Lett. **92**, 252001 (2004).
[29] K. P. Khemchandani, N. G. Kelkar, and B. K. Jain, Phys. Rev. C **68**, 064610 (2003); N. G. Kelkar, K. P. Khemchandani, and B. K. Jain, J. Phys. G **32**, L19 (2006).
[30] P. Kienle and T. Yamazaki, Phys. Lett. **B514**, 1 (2001); H. Geissel *et al.*, *ibid.* **549**, 64 (2002).
[31] K. Suzuki *et al.*, Phys. Rev. Lett. **92**, 072302 (2004).
[32] E. E. Kolomeitsev, N. Kaiser, and W. Weise, Phys. Rev. Lett. **90**, 092501 (2003).
[33] K. Tsushima, D. H. Lu, A. W. Thomas, and K. Saito, Phys. Lett. **B443**, 26 (1998).
[34] R. S. Hayano, S. Hirenzaki, and A. Gillitzer, Eur. Phys. J. A **6**, 99 (1999).
[35] D. Jido, H. Nagahiro, and S. Hirenzaki, Phys. Rev. C **66**, 045202 (2002); H. Nagahiro, D. Jido, and S. Hirenzaki, *ibid.* **68**, 035205 (2003).
[36] C. Garcia-Recio, J. Nieves, T. Inoue, and E. Oset, Phys. Lett. **B550**, 47 (2002); T. Inoue and E. Oset, Nucl. Phys. **A710**, 354 (2002).
[37] H. Nagahiro and S. Hirenzaki, Phys. Rev. Lett. **94**, 232503 (2005).
[38] S. D. Bass and A. W. Thomas, Phys. Lett. **B634**, 368 (2006).
[39] K. Saito, K. Tsushima, D. H. Lu, and A. W. Thomas, Phys. Rev. C **59**, 1203 (1999).
[40] F. Klingl, T. Waas, and W. Weise, Nucl. Phys. **A650**, 299 (1999).
[41] M. F. M. Lutz, G. Wolf, and B. Friman, Nucl. Phys. **A706**, 431 (2002); **A765**, 495 (2006).
[42] S. Hirenzaki, H. Nagahiro, T. Hatsuda, and T. Kunihiro, Nucl. Phys. **A710**, 141 (2002).
[43] H. Gilg *et al.*, Phys. Rev. C **62**, 025201 (2000); K. Itahashi *et al.*, *ibid.* **62**, 025202 (2000).
[44] H. Geissel *et al.*, Phys. Rev. Lett. **88**, 122301 (2002).
[45] Y. Umemoto, S. Hirenzaki, K. Kume, and H. Toki, Prog. Theor. Phys. **103**, 337 (2000); Phys. Rev. C **62**, 024606 (2000).
[46] C. Garcia-Recio, J. Nieves, and E. Oset, Phys. Lett. **B541**, 64 (2002).
[47] G. Chanfray, M. Ericson, and M. Oertel, Phys. Lett. **B563**, 61 (2003).
[48] E. Friedman and A. Gal, Phys. Lett. **B578**, 85 (2004).
[49] T. Schäfer, Phys. Rev. D **67**, 074502 (2003).
[50] D. J. Gross, R. D. Pisarski, and F. L. Yaffe, Rev. Mod. Phys. **53**, 43 (1981).
[51] R. D. Pisarski and F. Wilczek, Phys. Rev. D **29**, 338 (1984).
[52] R. Alkofer, P. A. Amundsen, and H. Reinhardt, Phys. Lett. **B218**, 75 (1989).
[53] J. Kapusta, D. Kharzeev, and L. D. McLerran, Phys. Rev. D **53**, 5028 (1996).
[54] E. V. Shuryak and M. Velkovsky, Phys. Rev. D **50**, 3323 (1994).
[55] T. Kunihiro, Phys. Lett. **B219**,363 (1989).
[56] K. Fukushima, K. Ohnishi, and K. Ohta, Phys. Rev. C **63**, 045203 (2001).
[57] P. Costa, M. C. Ruivo, and Yu. L. Kalinovsky, Phys. Lett. **B560**, 171 (2003); P. Costa, M. C. Ruivo, C. A. de Sousa, and Yu. L. Kalinovsky, Phys. Rev. D **70**, 116013 (2004).
[58] S. P. Klevansky, Rev. Mod. Phys. **64**, 649 (1992); T. Hatsuda and T. Kunihiro, Phys. Rep. **247**, 221 (1994); M. Buballa, *ibid.* **407**, 205 (2005).
[59] P. Rehberg, S. P. Klevansky, and J. Hüfner, Phys. Rev. C **53**, 410 (1996).
[60] P. Costa, M. C. Ruivo, C. A. de Sousa, and Yu. L. Kalinovsky, Phys. Rev. D **71**, 116002 (2005).
[61] G. W. Carter and D. Diakonov, Nucl. Phys. **A642**, c78 (1998); Phys. Rev. D **60**, 016004 (1999).
[62] H. Kiuchi and M. Oka, Prog. Theor. Phys. **114**, 813 (2005).
[63] A. Sibirtsev, Ch. Elster, S. Krewald, and J. Speth, AIP Conf. Proc. **717**, 837 (2004).
[64] K. Tsushima, Nucl. Phys. **A670**, 198c (2000).
[65] S. Hirenzaki, H. Toki, and T. Yamazaki, Phys. Rev. C **44**, 2472 (1991); H. Toki, S. Hirenzaki, and T. Yamazaki, Nucl. Phys. **A530**, 679 (1991).
[66] H. Toki and T. Yamazaki, Phys. Lett. **B213**, 129 (1988); H. Toki, S. Hirenzaki, T. Yamazaki, and R. S. Hayano, Nucl. Phys. **A501**, 653 (1989).
[67] E. Marco and W. Weise, Phys. Lett. **B502**, 59 (2001).
[68] S. Hirenzaki and E. Oset, Phys. Lett. **B527**, 69 (2002).
[69] H. Nagahiro, D. Jido, and S. Hirenzaki, Nucl. Phys. **A761**, 92 (2005).
[70] O. Morimatsu and K. Yazaki, Nucl. Phys. **A435**, 727 (1985); **A483**, 493 (1988).
[71] (SAPHIR Collaboration), Phys. Lett. **B444**, 555 (1998).
[72] W. T. Chiang, S. N. Yang, L. Tiator, M. Vanderhaeghen, and D. Drechsel, Phys. Rev. C **68**, 045202 (2003).
[73] N. Muramatsu (private communication).